Medicinal Chemistry Research (2019) 28:1818–1827
https://doi.org/10.1007/s00044-019-02408-3

MEDICINAL CHEMISTRY RESEARCH

ORIGINAL RESEARCH

Anxiolytic and anticonvulsant activity followed by molecular docking study of ceramides from the Red Sea sponge *Negombata sp*

Nermeen A. Eltahawy[1] · Amany K. Ibrahim[1] · Mohamed S. Gomaa[2] · Sawsan A. Zaitone[3,4] · Mohamed M. Radwan[5,6] · Hashim A. Hassanean[1] · Mahmoud A. ElSohly[2] · Safwat A. Ahmed[1]

Received: 30 March 2019 / Accepted: 19 July 2019 / Published online: 20 August 2019

Abstract

The chemical investigation of the Red Sea sponge *Negombata* sp. led to isolation and structure elucidation of five new ceramides *N* ((2S,3R,4*E*,8*E*)-1,3-dihydroxyhexacosa-4,8-dien-2-yl)pentadecanamide (**1**), *N*-((2S,3R,*E*)-1,3-dihydroxynonadec-4-en-2-yl)stearamide (**2**), *N*-[(2S,3R,*E*)-1,3 dihydroxyhexacos-4-en-2-yl]palmitamide (**3**), *N*-((2S,3R)-1,3-dihydroxydodecan-2-yl)tetradecanamide (**4**), *N*-[(2S,3S,4R)-1,3,4- trihydroxypentadecan-2-yl] palmitamide (**5**). Structure elucidation was achieved using spectroscopic techniques, including 1D and 2D NMR and HRMS. The isolated ceramides were tested for anti-anxiety action in the elevated plus maze and the light-dark transition box. Mice given diazepam or compounds number **1**, **2**, **3**, and **5** spent longer time in the light area of the light-dark box. However, compound **4** did not produce a similar effect. Similarly, testing anti-anxiety action in the elevated plus maze test showed that the compounds number **2**, **3**, and **5** or diazepam were able to prolong the open arm time %. Meanwhile, compounds **1** and **4** failed to produce a similar response. In addition, the anticonvulsant action of the ceramides was assessed employing pentylenetetrazole-induced seizures, where some ceramides prolonged the time to death due to pentylenetetrazole in vivo. In silico testing of the isolated ceramides displayed reasonable GABA receptor modulator binding at the benzodiazepines site. Ceramide 1 showed slightly stronger interaction with the GABA receptor over other ceramides which is compatible with the results of their anxiolytic activity.

Keywords *Negombata sp.* · Ceramide · Anticonvulsant · Anxiolytic · Molecular modeling

Introduction

Many studies show that natural products have great potential for the treatment of vast array of diseases (Izumi et al. 2012). These products are rich in secondary metabolites, as terpenes, steroids, polyketides, peptides, alkaloids, and porphyrins (Torres et al. 2014). Recently, various bioactive compounds have been isolated from many marine organisms such as tunicates, sponges, soft corals, sea hares, nudibranchs, bryozoans, sea slugs, and marine organisms (Eltahawy et al. 2015).

Sponges are important to the overall ecology of coral reefs for many reasons: they are very efficient filter feeders, providing an important link in benthic–pelagic coupling, they appear to be capable of absorbing dissolved organic carbon as a food source, and their bodies provide shelter for large numbers of invertebrates and fish. An enormous array of antitumor, antiviral, antiinflammatory, immunosuppressive, antibiotic, and other bioactive molecules that can affect the pathogenesis of many human diseases are produced from marine sponges (Sipkema et al. 2005).

Supplementary information The online version of this article (https://doi.org/10.1007/s00044-019-02408-3) contains supplementary material, which is available to authorized users.

✉ Safwat A. Ahmed
safwat_aa@yahoo.com

[1] Department of Pharmacognosy, Faculty of Pharmacy, Suez Canal University, Ismailia, Egypt

[2] Chemistry Department, College of Clinical Pharmacy, Imam Abdulrahman Bin Faisal University, Dammam, Saudi Arabia

[3] Department of Pharmacology & Toxicology, Faculty of Pharmacy, Suez Canal University, Ismailia, Egypt

[4] Department of Pharmacology & Toxicology, Faculty of Pharmacy, University of Tabuk, Tabuk, Saudi Arabia

[5] National Center for Natural Products Research, School of Pharmacy, University of Mississippi, University, Mississippi, MS 38677, USA

[6] Faculty of Pharmacy, Pharmacognosy Department, Alexandria University, Alexandria, Egypt

Table 1 ^{1}H (400 MHz) and ^{13}C (100 MHz) NMR spectroscopic data of ceramides 1–3 in $CDCl_3$

Compound 1			Compound 2			Compound 3		
Position	δ_C	δ_H	Position	δ_C	δ_H	Position	δ_C	δ_H
1	62.4	2H, 3.64 (br d)	1	62.4	2H, 3.89 (dd, 8.0, 4.8)	1	62.7	2H, 3.83 (dd, 8.0, 4.8)
2	54.5	1H, 3.88 (m)	2	54.5	1H, 4.29 (m)	2	54.7	1H, 4.30 (m)
3	74.5	1H, 4.30 (m)	3	74.5	1H, 3.67 (m)	3	74.8	1H, 3.70 (m)
4	129.0	1H, 5.47 (dd, 15.0, 6.10)	4	128.8	1H, 5.50 (dd, 15.0, 6.10)	4	129.0	1H, 5.52 (dd, 15.0, 6.10)
5	129.0	1H, 5.77 (dt, 15.0, 7.0)	5	134.2	1H, 5.77 (dt, 15.0, 7.0)	5	134.5	1H, 5.79 (dt, 15.0, 7.0)
6	32.3	2H, 2.05 (dt, 21.1, 6.5)	6	31.9	2H, 2.03 (m)	6	32.2	2H, 2.05 (m)
7	32.3	2H, 2.05 (dt, 21.1, 6.5)	7–14	29.7	2H, 1.24 (m)	7-10′	29.9	2H, 1.25 (m)
8	134.2	1H, 5.47 (dt, 14.7, 10.0)	15	29.1	2H, 1.24 (m)	11	29.3	2H, 1.25 (m)
9	131.3	1H, 5.47 (dt, 14.7, 10.0)	16	36.9	2H, 1.24 (m)	12	37.1	2H, 1.25 (m)
10	31.9	2H, 2.05 (dd,10.3, 6.8)	17	31.9	2H, 1.24 (m)	13	32.2	2H, 2.13 (m)
11–22	29.7	2H, 1.24 (m)	18	22.7	2H, 1.24 (m)	14	22.9	2H, 2.13 (m)
23	39.0	2H, 1.24 (m)	19	14.1	3H, 0.87 (t, 6.8)	15	14.4	3H, 0.89 (t, 6.8)
24	31.9	2H, 1.24 (m)	1′	174.0		1′	174.2	
25	22.7	2H, 1.24 (m)	2′	36.8	2H, 2.21 (t, 7.6)	2′	37.1	2H, 2.22 (t, 7.6)
26	14.1	3H, 0.86 (t, 6.8)	3′	25.8	2H, 1.61 (m)	3′	26.0	2H, 1.62 (m)
1′	173.0		4′-15′	29.7	2H, 1.24 (m)	4′-13′	29.7	2H, 1.25 (m)
2′	37.0	2H, 2.21 (t, 7.6)	16′	32.3	2H, 1.24 (m)	14′	32.5	2H, 1.25 (m)
3′	25.9	2H, 1.60 (m)	17′	22.7	2H, 1.24 (m)	15′	22.9	2H, 1.25 (m)
4′–12′	29.7	2H, 1.24 (m)	18′	14.1	3H, 0.87 (t, 6.8)	16′	14.4	3H, 0.89 (t, 6.8)
13′	31.9	2H, 1.24 (m)	NH		6.32(d, 8.4)	NH		6.33
14′	22.7	2H, 1.24 (m)						
15′	14.1	3H, 0.86 (t, 6.8)						
NH		6.31 (d, 8.4)						

Marine environment from Red Sea, being one of the most biodiverse in the world, offers a potential for producing new drugs and prototypes. Some studies about chemical constituents of the marine sponge *Negombata sp*. were done. Latrunculins (Ahmed et al. 2005), terpines (Chao et al. 2010), lipids, and sterols (Ahmed et al. 2006) have been isolated from the sponge *Negombata*. A ceramide mixture (antiepileptic) was isolated from sponge *Negombata corticata*. Collected from the Red Sea. Extensive spectroscopic analysis was done to know the chemical structures of the metabolites (Ahmed et al. 2008).

Here, we report the isolation and identification of five unknown ceramides (**1**, **2**, **3**, **4**, and **5**) and in vivo evaluation of their anticonvulsant and anxiolytic activity.

Materials and methods

General

Spectra (^{1}H NMR (400 MHz), ^{13}C NMR (100 MHz), DEPT-135, and 2D-NMR) were done using the residual solvent signal as an internal standard on a Varian AS 400. A Bruker Tensor 27 was used to measure the IR spectra. A Bruker BioApex was used to measure high resolution mass spectra.

Hewlett Packard gas liquid chromatography (HP), series model 6890 equipped with Flame Ionization Detector was used to identify fatty acid methyl esters. In addition, a capillary column (HP-INNOWAX, Polyethylene Glycol, 30 m × 530 µm, film thickness 1.00 µm) was used in fatty acids' separation. The temperature of the injector port was set at 250 °C (splitless mode) and 14.81 psi for pressure also, the detector cell at 275 °C. The carrier gas(N_2)'s flow rate was adjusted at 30 mL/min. The initial column temperature was 70 °C and increased to 200 °C by the rate of 4 °C/min, then isothermally for a total run time of 32.5 min.

Thin layer chromatography (20 × 20 cm) (E. Merck) was done using pre coated silica gel G-25 UV_{254} plates. Flash column chromatography (Whatman) was done using Silica gel Purasil 60A, 230–400 mesh.

Collection and identification of the animal organism

The *Negombata* sp. sponge was collected using SCUBA by hand from Safaga. The sponge material was frozen

immediately and kept frozen at −20 °C until processed. The voucher specimen was deposited at the Zoological Museum of the University of Amsterdam under registration No. ZMAPOR. **19755**. and in the Egyptian Red Sea invertebrates collection at the Pharmacognosy department with registration numbers (SAA-1). The identification and description of the sponge was provided by Prof. Rob. W.M. van Soest, at the Institute for Systematic and Ecology, The University of Amesterdam, Amesterdam, Netherlands.

Extraction, fractionation, and isolation

Negombata sp. (350 g) was dried, grounded, and extracted using a mixture of MeOH/CH_2Cl_2 (1:1) (3 × 2 L) at the room temperature. Hundred grams residue was obtained from the extract after evaporated under vacuum hexane, EtOAc and MeOH gradient on a flash silica gel was used on the vacuum liquid chromatography to give five fractions from the extract. One of these fractions was subjected to silica gel column chromatography eluted initially with 20% EtOAc in hexane followed by gradient systems of n-hexane and EtOAc. The effluent was collected in fractions (20 mL each), where three subfractions (3a, 3b, and 3c) were obtained. The isolated ceramides were obtained from these fractions after further purification on Sephadex LH-20 column.

The ceramide hydrolysis

Three milligrams of each compound was heated separately in 15 mL of MeOH with 5 mL of 1 M HCl for 4 h at 90 °C. The mixture was extracted with hexanethen, the hexane layer was concentrated under vacuum to give the hydroxyl fatty acid methyl esters of **2** and **3**, while in the case of compounds **1**, fatty acid methyl ester was obtained. Lemieux oxidation was then used for the separation of the hydroxyl fatty acid methyl esters of **2** and **3** (Sun et al. 2006; Kuksis 1978; Lemieux and Von rudlo 1955). In this previous reaction, 0.09 mol/L $NaIO_4$ (2.0 mL), 0.023 mol/L aqueous $KMnO_4$, *t*-BuOH (1.0 mL), and 0.04 mol/L aqueous K_2CO_3 (0.5 mL) were slowly added to the hydroxyl fatty acid methyl ester of compounds **2** and **3**. The mixtures were then stirred for 24 h at room temperature, quenched with 0.5 mL of 2.5 mol/L H_2SO_4 and saturated aqueous Na_2SO_3, and then extracted with Et_2O (5 × 3 mL). After that the organic layer was dried over Na_2SO_4. Finally, the dried, concentrated residue was esterified with excess CH_2N_2 in Et_2O overnight. GC-MS was used to analyze the resulting esters.

Isolates

N-((2S,3R,4E,8E)-1,3-dihydroxyhexacosa-4,8-dien-2-yl) pentadecanamide (**1**): White powder; HR-ESI-MS (negative ion mode) *m/z* 632.5838 [M–H]- (calcd. for $C_{41}H_{79}NO_3$:632.5982); ^{1}H NMR and ^{13}C NMR spectral data see Table 1.

N-((2S,3R,4E)-1,3-dihydroxynonadec-4-en-2-yl)stearamide (**2**): White powder; HR-ESI-MS (positive ion mode) *m/z* 580.5682 $[M + H]^+$ (calcd for $C_{37}H_{73}NO_3$:580.5669); ^{1}H NMR and^{13}C NMR spectral data see Table 1.

***N*-[(2S,3R,4*E*)-1,3-dihydroxyhexacos-4-en-2-yl]** palmitamide (**3**): White powder; HR-ESI-MS (positive ion mode) *m/z* 518.4512 [M + Na] + (calcd for $C_{31}H_{61}NNaO_3$:518.4549); ^{1}H NMR and ^{13}C NMR spectral data see Table 1.

N-((2S,3R)-1,3-dihydroxydodecan-2-yl)tetradecanamide (**4**): White powder; HR-ESI-MS (negative ion mode) *m/z* 426.3880 $[M–H]^-$ (calcd for $C_{26}H_{52}NO_3$:426.3947); ^{1}H NMR and ^{13}C NMR spectral data see Table 2.

***N*-[(2S,3S,4R)-1,3,4- trihydroxypentadecan-2-yl] palmitamide** (**5**): White powder; HR-ESI-MS (positive ion mode) *m/z* 536.4544 $[M + Na]^+$ (calcd. for $C_{31}H_{63}NNaO_4$:536.4655); ^{1}H NMR and ^{13}C NMR spectral data see Table 2.

Table 2 ^{1}H (400 MHz) and ^{13}C (100 MHz) NMR spectroscopic data of ceramides 4–5 in C_5D_5N

Compound 4			Compound 5		
Position	δ_C	δ_H	Position	δ_C	δ_H
1	62.3	2H, 4.52 (dd, 8.0, 4.8)	1	62.1	2H, 4.54 (dd, 8.0, 4,8)
2	53.2	1H, 5.13 (m)	2	53.0	1H, 5.13 (m)
3	77.0	1H, 4.45 (m)	3	76.8	1H, 4.46 (m)
4	34.4	2H, 1.32 (m)	4	73.1	1H, 4.30 (m)
5	30.7	2H, 1.32 (m)	5	34.2	2H, 1.28 (m)
6	28.5	2H, 1.32 (m)	6	26.8	2H, 1.28 (m)
7	30.3	2H, 1.32 (m)	7–9	30.2	2H, 1.28 (m)
8	30.5	2H, 1.32 (m)	10	30.2	2H, 1.28 (m)
9	39.6	2H, 1.32 (m)	11	28.0	2H, 1.28 (m)
10	30.6	2H, 1.32 (m)	12	37.4	2H, 1.28 (m)
11	27.0	2H, 1.32 (m)	13	28.3	2H, 1.28 (m)
12	14.6	3H, 0.90 (t, 6.8)	14	23.1	2H, 1.28 (m)
1′	175.5		15	14.4	3H, 0.89 (t, 6,8)
2′	36.0	2H, 2.26 (t, 7.6)	1′	175.3	
3′	28.1	2H, 1.96 (m)	2′	35.8	2H, 2.25 (t, 7.6)
4′-11′	30.3	2H, 1.32 (m)	3′	25.9	2H, 1.97 (m)
12′	32.5	2H, 1.32 (m)	4′-13′	30.2	2H, 1.28 (m)
13′	26.1	2H, 1.32 (m)	14′	32.2	2H, 1.28 (m)
14′	14.6	3H, 0.90 (t, 6,8)	15′	22.9	2H, 1.28 (m)
NH		8.59 (d, 8.4)	16′	14.4	3H, 0.89 (t, 6.8)
			NH		8.61 (d, 9.2)

Anxiolytic activity

The anxiolytic activity of the isolated ceramides was investigated using two well documented animal (mouse) paradigms for anxiety; the first one was the light-dark transition test and the second one was the elevated plus maze (EPM). A dose of diazepam known to induce anxiolytic-like effect in mice (Naderi et al. 2008) was utilized as a standard medication.

Effect of the test compounds on anxiety behavior

Animal experiment was approved by the research ethics committee at Faculty of Pharmacy, Suez Canal University. Albino Swiss mice were habituated to the testing room undisturbed for at least 2 h before experimentation. Thirty minutes following i.p. injection of the test compounds, mice were gently handled from the home cages and put individually in the paradigm. Then, mice were placed on the central point of the EPM while their faces directed toward one of the open arms. The testing time was set as three minutes and was video-recorded. Cleaning of the maze was done after each session by 10% alcohol followed by a dry cloth in order to remove any olfactory cues (e.g., urine and/or fecal matter) from the surface of the apparatus. Later, the recorded videos of the sessions were analyzed for anxiety-like behavior.

Behavioral parameters comprised both conventional spatio-temporal measures (Holmes and Rodgers 1998; Rodgers et al. 2003). The measurements determined from the videos were the number of times of arm entries (arm entry = all four paws into an open or a closed arm). In addition, the time spent in open and closed arms of the maze were measured. Time of exploring the open arm was considered as a measure of antianxiety action (Pellow et al. 1985).

Open arm exploration was characterized by two variables: the percent of time spent in open arms of the maze [(%OAT = time in open arms/(time in open arms + time in closed arms)]. The increase in both %OAT has been shown to be an index of lowered anxiety-like behavior. Any mouse fell off an open arm was omitted from calculations.

Anticonvulsant activity: effect of the test compounds on time to death due to pentylenetetrazole

An acute dose of PTZ (70 mg/kg, i.p.) was utilized for induction of death. The capability of the compounds to extend the time to death due to PTZ was considered an indication toward anticonvulsant action. The compounds were evaluated and compared to the standard drug, diazepam. The control group was injected with DMSO (the vehicle of the test compounds) 30 min prior to PTZ injection. The time to death was recorded and compared.

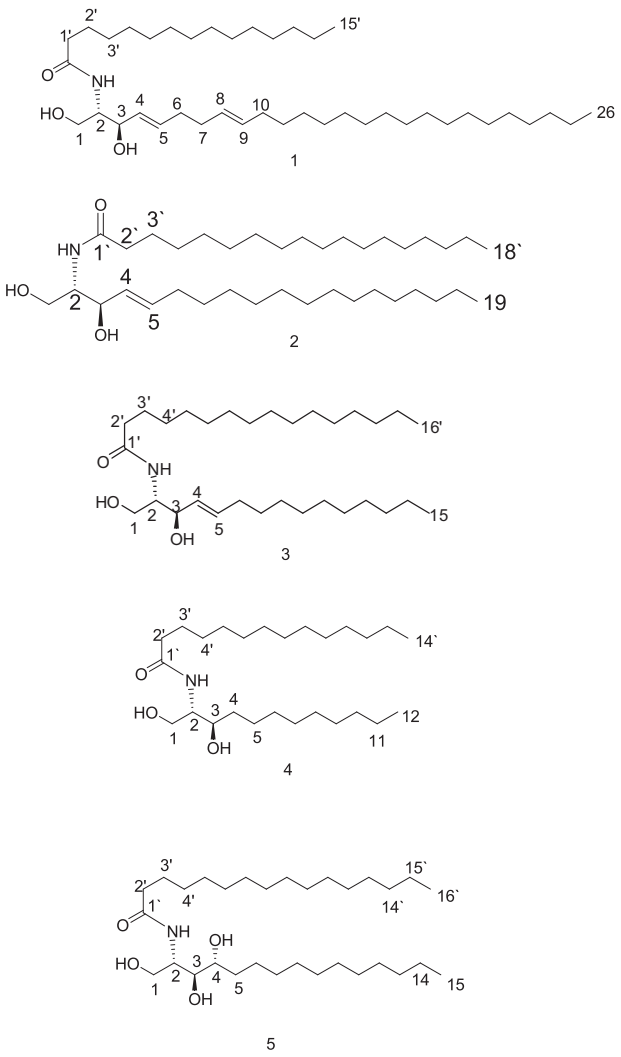

Fig. 1 Chemical structure for compounds 1, 2, 3, 4, and 5

Data analysis and statistics

Data were presented as mean ± S.E. of the mean. One-way ANOVA was employed followed by Bonferroni's *post hoc* test. These tests were applied using the Statistical Package for Social Sciences (SPSS Inc., USA). *P* value less 0.05 was set as the accepted level of significance.

Molecular modeling

All molecular modeling studies were performed on a Hewlett-Packard Pentium Dual-Core T4300 2.10 GHz running Windows 10 using molecular operating environment (MOE) 2008.10 molecular modeling software for molecular docking simulation and ligand binding energy calculation

and Molsoft ICM-Pro 3.5-0 for output data visualization. The X-ray crystal structure of a pentameric ion channel gated with a ligand from Erwinia chrysanthemi (ELIC) in complex with GABA and flurazepam (PDB code 2YOE) was used as the target receptor. The selected target was used after deleting the co-crystallized ligand and then docking was performed using MOE dock tool in MOE, performed with the default values. The amino acid residues involved in binding the co-crystallized ligand was used to define the active site for ligands binding.

The docking results were evaluated visually through interaction with key residues and has been calibrated using crystallized ligand by checking ligand binding position.

Results and discussion

Five new compounds were isolated (Fig. 1), and analyzed with different spectral data. Herein, we describe the structure elucidation for the five compounds.

Compound **1** was obtained as a white powder, and its molecular formula was determined to be $C_{41}H_{79}NO_3$ by HRESIMS *m/z* 632.5838 $[M–H]^-$ (calcd 632.5982), representing three degrees of unsaturation. The ^1H and ^{13}C–NMR spectral data of compound **1** are listed in Table 1.

The ^1H-NMR spectrum, in Table 1, showed resonances of an amide proton doublet at δ_H 6.31 (d, $J = 8.4$ Hz) and protons of long methylene chain at δ_H 1.24, indicating a sphingolipid skeleton. In addition, characteristic resonances of a 2-amino-1,3-diol unit of the hydrocarbon chain were observed at δ_H 3.88 (t, $J = 6.8$ Hz), 4.30 (m) and 3.64 (brd) assigned for H-2, H-3, and H_2-1 respectively and also resonances for four olefinic protons at δ_H 5.47 (dd, $J = 15.0$, 6.10 Hz) assigned for (H-4, H-8, and H-9) and δ_H5.77 (dt, $J = 15.0$, 7.0) assigned for H-5.Moreover, resonances of aliphatic hydrocarbons at δ_H 0.86 (t, $J = 6.8$ Hz) assigned for H-26 and H-15′, 1.24 (overlapped H, m), 2.21 (t, $J =$ 7.6 Hz) assigned for H-2′ and 1.60 (m) assigned for H-3′.

The ^{13}C-NMR spectrum, in Table 1, showed resonances of 41 carbon atoms. Characteristic resonances of a 2-amino-1,3-triol unit of the hydrocarbon chain were observed at δ_C 62.4 (C-1), 54.5 (C-2), and 74.5 (C-3). In addition, there are four olifinic carbons' resonances at δ_C 129.0 (C-4), and (C-5), 134.2 (C-8), and 131.3 (C-9). Also, the two terminal methyl groups (C-26 and C-15′) showed a resonance at δ_C 14.1 and the amide carbonyl (C-1′) at δ_C173.0.

The ^1H–^1H COSY spectrum confirmed the position of the double bonds between H-4/H-5, H-5/H_2-6, H_2-6/H_2-7, H_2-7/H-8, and H-8/H-9 and also from HMBC of H-4/C-5 ($^2J_{CH}$), H-4/C-6 ($^3J_{CH}$), H-5/C-6 ($^2J_{CH}$), H-5/C-7 ($^3J_{CH}$), $H_2$6/C-8 ($^3J_{CH}$), H_2-7/C-8 ($^2J_{CH}$), H_2-7/C-9 ($^3J_{CH}$), H-8/C-9 ($^2J_{CH}$) leading to assignment of the carbons C-4/C-5/C-6/C-7/C-8/C-9.

The position and geometry of the double bonds were confirmed by ^1H–^1H COSY analysis and coupling constant data. The $J_{4,5}$ (15.0 Hz) and $J_{8,9}$ (14.7 Hz) values indicates the trans geometry of the double bonds. Furthermore, the presence of the δ_C 32.3 (C-6) and 31.9 (C-10) prove that the geometry of the double bonds is 4E, 8E-sphingadiene type ceramide as the geometry of the double bond in a long chain alkene can be determined from the ^{13}C-NMR chemical shift of the methylene carbon atom next to the olefinic carbon atom. The carbon signal is observed near to 27 in the (*Z*) type and near to 32 in the (*E*) type (Inagakia et al. 1998). Therefore, 1 was assigned as a new 4*E*, 8*E*-sphingadiene type ceramide.

The GC-MS analysis of fatty acid methyl ester of compound **1** was performed after hydrolysis, that showed a molecular ion peak of *m/z* (256)on the chromatogram corresponding to a C_{16} fatty acid methyl ester that indicated the presence of one terminal fatty acid hexadecanoic ($C_{16:0}$) acid.

As reported in the literature, comparison of the physical data of ^1H NMR and ^{13}C NMR with analogs was done to assign the configuration of the ceramide moieties which indicated the absolute configurations of C-2 and C-3 to be 2S and 3R, respectively (Kwon et al. 1991).

Compound 2 was obtained as white powder, and its molecular formula was determined to be $C_{37}H_{73}NO_3$ by HRESIMS *m/z* 580.5682 $[M + H]^+$ (calcd. 580.5669), indicating two degrees of unsaturation. The ^1H and ^{13}C-NMR spectral data of compound **2** are listed in Table 1.

The ^1H-NMR spectrum, in Table 1, showed resonances of an amide proton doublet at δ_H6.32 (d, $J = 8.4$ Hz) and protons of long methylene chain at δ_H1.24, that indicats a sphingolipid skeleton. In addition, characteristic resonances of a 2-amino-1,3-diol unit of the hydrocarbon chain were observed at δ_H 3.89 (dd, $J = 8.0$, 4.8 Hz), 4.29 (m) and 3.67 (m) assigned for H-1, H-2, and H-3 respectively (Kwon et al. 1991). Resonances for two olefinic protons at δ_H 5.50 (dd, $J = 15.0$, 6.1 Hz) and 5.77 (dt, $J = 15.0$, 7.0 Hz) assigned for H-4 and H-5. Also, resonances for aliphatic hydrocarbons at δ_H 0.87 (t, $J = 6.8$ Hz) assigned for H-19 and H-18′, 2.21 (t, $J = 7.6$ Hz) assigned for H-2′, 1.24 (overlapped H, m) and 1.61 (m) assigned for H-3′ were observed.

The ^{13}C-NMR spectrum, in Table 1, showed resonances of 37 carbon atoms. Characteristic resonances of a 2-amino-1,3-diol unit of the hydrocarbon chain were observed at δ_C 62.4 (C-1), 54.5 (C-2), and 74.5 (C-3) (Kwon et al. 1991). Moreover, there are two resinances for olifinic carbons at δ_C128.8 (C-4) and 134.2 (C-5). Also, a resonance at δ_C 14.1 assigned for the two terminal methyl groups (C-19 and C18′) and a resonance at δ_C174.0 assigned for the amide carbonyl (C-1′) were observed.

The position of the double bonds was confirmed through the ^1H–^1H COSY spectrum as there were correlations between H-4/H-5, H-5/H_2-6, as well as the HMBC spectrum

which showed correlations from H-4/C-5 ($^2J_{CH}$), H-4/C-6 ($^3J_{CH}$), H-5/C-6 ($^2J_{CH}$), H-5/C-7 ($^3J_{CH}$) leading to assignment of the C-4/C-5 double bond. The position and geometry of the double bond was confirmed by ^{1}H–^{1}H COSY analysis and coupling constant data. The (15.0 Hz) $J_{4,5}$ value indicated the *trans* geometry of this double bond. Furthermore, the presence of (C-6) at δ_C 31.9 proves that the double bond geometry is 4E sphingadiene type ceramide and the double bond geometry in a long chain alkene can be proved from the ^{13}C-NMR chemical shift of the methylene carbon atom next to the olefinic carbon atom. The carbon signal is observed near to 27 in the (*Z*) type and near to 32 in the (*E*) type (Inagakia et al. 1998), so, compound 2 was assigned as a ceramide of 4*E* sphingadiene type.

The GC-MS analysis of fatty acid methyl ester of 2 was done after hydrolysis, which exhibited a molecular ion peak of *m/z* (298) on the chromatogram which is related to a C_{19} fatty acid methyl ester indicating the presence of octadecanoic ($C_{18:0}$) acid which is one terminal fatty acid.

Comparison of the physical data, ^{1}H NMR and ^{13}C NMR with analogs as reported in the literature was done to assign the configuration of the ceramide moieties, that proved the absolute configurations of C-2 and C-3 to be 2S and 3R, respectively (Kwon et al. 1991).

Compound **3** was obtained as white powder, and its molecular formula was determined to be $C_{31}H_{61}NNaO_3$ by HRESIMS *m/z* 518.4512 $[M+Na]^+$ (calcd 518.4549), representing two degrees of unsaturation. The ^{1}H and ^{13}C-NMR spectral data of compound **3** are listed in Table 1.

The ^{1}H-NMR spectrum, in Table 1, showed resonances of an amide proton doublet at δ_H 6.33 (NH) and protons of a long methylene chain at δ_H 1.25, that indicated a sphingolipid skeleton. In addition, a 2-amino-1,3-diol unit characteristic resonances of the hydrocarbon chain were observed at δ_H 3.83 (dd, $J = 8.0$, 4.8 Hz), 4.30 (m), and 3.70 (m) assigned for H-1, H-2, and H-3 respectively (Kwon et al. 1991) and two olefinic protons' resonances at δ_H 5.52 (m, H-4) and 5.79 (m, H-5), assigned for H-4 and H-5. Also, resonances corresponding to aliphatic hydrocarbons at δ_H 0.89 (t, $J = 6.8$ Hz) assigned for H-15 and H-16′, 1.25 (overlapped H, m), 1.62 (m) assigned for H-3′ and 2.22 (t, $J = 7.6$ Hz) assigned for H-2′.

The ^{13}C-NMR spectrum, in Table 1, showed resonances of 31 carbon atoms. A 2-amino-1,3-diol unit characteristic resonances of the hydrocarbon chain were observed at δ_C 54.5 (C-2), 62.4 (C-1) and 74.5 (C-3) (Kwon et al. 1991). Also, there is a resonance at δ_C 14.1 assigned for the two terminal methyl groups (C-15 and C-16′) and at δ_C 174.0 assigned for the amide carbonyl (C-1′).

The ^{1}H–^{1}H COSY spectrum confirmed the position of the double bondsas there were correlations between H-4/H-5, H-5/H_2-6 leading to assignment of the double bond between C-4 and C-5.

The spectral data of **3** were compared with **2** which showed a close resemblance leading to the identification of the position and geometry of the double bond as a 4*E* sphingadiene type. The (15.0 Hz) of $J_{4,5}$ value indicated the *trans* geometry of this double bond. Furthermore δ_C 32.2 (C-6) proofs that the geometry of the double bonds is 4E sphingadiene type ceramide and the double bond geometry in a long chain alkene can be determined from the ^{13}C-NMR chemical shift of the methylene carbon atom next to the olefinic carbon atom. The carbon signal is observed near to 27 in the (*Z*) type and near to 32 in the (*E*) type (Inagakia et al. 1998). So, compound 3 was assigned as ceramide of a 4*E* sphingadiene type.

The GC-MS analysis of fatty acid methyl ester of 3 was done after hydrolysis, which showed a molecular ion peak of *m/z* (270) on the chromatogram which corresponds to a C_{16} fatty acid methyl ester indicating the presence of only one terminal fatty acid, palmitic acid ($C_{16:0}$).

Comparison of the physical data, ^{1}H NMR and ^{13}C NMR with analogs as reported in the literature was done to assign the configuration of the ceramide moieties, which indicated the absolute configurations of C-2 and C-3 to be 2S and 3R, respectively (Kwon et al. 1991).

Compound 4 was obtained as white powder, and its molecular formula was determined to be $C_{26}H_{52}NO_3$ by HRESIMS *m/z* 426.3880 $[M-H]^-$ (calcd 426.3947), representing one degree of unsaturation. The ^{1}H and ^{13}C-NMR spectral data of compound **4** are listed in Table 2.

The ^{1}H-NMR spectrum, in Table 2, showed resonances of an amide proton doublet at δ_H 8.59 (d, $J = 8.4$ Hz) and a long methylene chain protons at δ_H 1.32, indicating a sphingolipid skeleton. In addition, a 2-amino-1,3-diol unit's characteristic resonances of the hydrocarbon chain were observed at δ_H 5.13 (m), 4.52 (dd, $J = 8.0$, 4.8 Hz) and 4.45 (m) to be assigned for H-2, H_2-1 and H-3 respectively (Kwon et al. 1991). Also, resonances corresponding to aliphatic hydrocarbons at δ_H 0.90 (t, $J = 6.8$ Hz) assigned for H-12 and H-14′, 1.96 (m) assigned for H-3′, 1.32 (overlapped H, m) and 2.26 (t, $J = 7.6$ Hz) assigned for H-2′.

The ^{13}C-NMR spectrum, in Table 2, showed resonances of 26 carbon atoms. A 2-amino-1,3-diol unit characteristic resonances of the hydrocarbon chain were observed at δ_C 53.2 (C-2), 62.3 (C-1) and 77.0 (C-3). Also, a resonance at δ_C 14.6 assigned for the two terminal methyl groups (C-12 and C-14′) and a resonance at δ_C 175.5 assigned for the amide carbonyl (C-1′) were found (Kwon et al. 1991).

The GC-MS analysis of fatty acid methyl ester of compound **4** was carried out after hydrolysis, which exhibited a peak at molecular ion of *m/z* (242) on the chromatogram corresponding to a C_{14} fatty acid methyl ester which indicated the presence of one terminal fatty acid myrstic ($C_{14:0}$) acid.

The chemical shifts of C-2 (δ54.0) and C-3 (δ76.8) were very similar to those of the neurotrophic ceramide

(4E,6E,2S,3R) -2-N-eicosanoyl-4,6-tetradecasphingadienine (Kwon et al. 1991). This evidence proved the absolute configurations at C-2 and C-3 to be 2S and 3R, respectively.

Compound 5 was obtained as a white powder, and its molecular formula was determined to be $C_{31}H_{63}NNaO_4$ by HRESIMS *m/z* 536.4544 $[M + Na]^+$ (calcd. 536.4655), representing one degree of unsaturation. The ^1H and ^{13}C-NMR spectral data of compound **5** are listed in Table 2.

The ^1H-NMR spectrum, Table 1, exhibited resonances of an amide proton at δ_H 8.61 (d, $J = 9.2$ Hz) and a long methylene chain protons at δ_H1.28, indicating a sphingolipid skeleton. In addition, a 2-amino-1,3,4-triol unit characteristic resonances of the hydrocarbon chain were observed at δ_H 5.13 (m), 4.54 (dd, $J = 8.0$, 4.8 Hz), 4.46 (m) and 4.30 (m) assigned for H-2, H-1, H-3 and H-4 respectively. Also, there were resonances corresponding to aliphatic hydrocarbons at δ_H 0.89 (t, $J = 6.8$ Hz) assigned for H-15 and H-16′, 1.28 (overlapped H, m), 1.97 (m) assigned for H-3′ and 2.25 (t, $J = 7.6$ Hz) assigned for H-2′.

The ^{13}C-NMR spectrum, in Table 2, showed resonances of 31 carbon atoms. A 2-amino-1,3,4-triol unit Characteristic resonances of the hydrocarbon chain were observed at δ_C 53.0 (C-2), 62.1 (C-1), 76.8 (C-3), and 73.1 (C-4). Also, a resonance at δ_C 14.4 assigned for the two terminal methyl groups (C-15 and C-16′) and at δ_C 175.3 assigned for the amide carbonyl (C-1′) were observed.

The ^1H–^1H COSY correlations, between H_2-1/H-2, H-2/H-3, H-3/H-4, and H-4/H_2-5 and also the HMBC correlations, of H_2-1/C-2 ($^2J_{CH}$), H_2-1/C-3 ($^3J_{CH}$), H-2/C-3 ($^2J_{CH}$), H-3/C-2 ($^2J_{CH}$), H-3/C-4 ($^2J_{CH}$), H-4/C-2 ($^3J_{CH}$), H-4/C-6 ($^3J_{CH}$) confirms the positions of the hydroxyl groups, leading to assignment of C-1/C-2/C-3/C-4.

GC-MS analysis of the fatty acid methyl ester of compound **5** was done after hydrolysis, which showed a molecular ion peak of *m/z* (270) on the chromatogram that corresponds to a C_{17} fatty acid methyl ester indicating the presence of just one terminal fatty acid palmitic acid ($C_{16:0}$).

Comparison of the physical data, ^1H NMR and ^{13}C NMR with analogs reported in the literature was done to confirm the configuration of the ceramide moieties which indicated the absolute configurations of C-2, C-3, and C-4 to be 2S, 3S, and 4R, respectively (Sugiyama et al. 1991).

In vivo evaluation of the anxiolytic and anticonvulsant activity

Anxiolytic effect was inspected by the light-dark transition box; in which we measured the time spent in the light area which reflects relaxation and comfort in a light area that is originally considered aversive by the mice. In the EPM test, anxiety-like behavior was expressed in terms of percentage time consumed in the two open arms (%OAT).

Most neurodegenerative diseases are associated with changes in sphingolipid composition in a variety of cell types in the nervous system (Wang and Beibrich 2018). For instance, in PD dementia, elevated ceramides was linked to memory dysfunction (Xing et al. 2016). Furthermore, ceramides have been linked to multiple pathophysiological mechanisms of depression including neurodegeneration and elevated inflammation (Bieberich 2012; Kornhuber et al. 2014). Physiologically, sphingolipids undergo vital cell signaling in cellular membranes and susceptible to enzymatic hydrolysis. Many sphingolipids are precursors as well as derivatives of other types of sphingolipids, it not clear which specific type is linked to a disease and whether it is contributing to the pathology of a disease (Wang and Beibrich 2018). Sphingolipids, in particular ceramides, have been suggested as a novel therapeutic target for depression due to their potential roles in its pathophysiology (Kornhuber et al. 2014). One previous study, highlighted anti-epileptic activity for some ceramides from Red Sea soft coral Sarcophyton auritum. The study concluded that the mechanism of action includes GABA-A agonistic activity (Eltahawy et al. 2015). Furthermore, the in vitro effect of ceramide was tested in one ischemia model in SH-SY5Y neuroblastoma cells. A dual effect of ceramide was observed, depending on ceramide concentration. The authors concluded that although deviations in the metabolism of ceramide have been linked to tissue injury in case of brain ischemia (Kubota et al. 1996) and heart ischemia in rats (Beresewicz et al. 2002) and there is evidence for the role of ceramide in apoptosis, it is additionally plays a key role in the process of cytoprotection, such as preconditioning (Lecour et al. 2006; Cui et al. 2004).

Anxiolytic activity

Testing of the anxiolytic activity for the tested compounds versus diazepam in the light-dark box showed different values for time spent in the light area. Administration of diazepam at 1 mg/kg, i.p.) or compounds **1**, **2**, **3**, and **5** prolonged the time spent within the light area of the light-dark box however; compound **4** did not produce a similar effect (Fig. 2). Similarly, screening of the anxiolytic activity of the test compounds in the elevated plus maze indicated that the test compounds **2**, **3**, and **5** as well as diazepam (1 mg/kg) prolonged the open arm time % in comparison to mice treated with the vehicle (Fig. 3).

Diazepam is a standard medication from the benzodiazepine group that acts by agonistic action on GABA-A receptors. Stimulation of these receptors leads to opening of chloride channels and membrane hyperpolarization. The net result is always CNS depression. Diazepam is used medicinally for alleviating anxiety disorders and panic attacks.

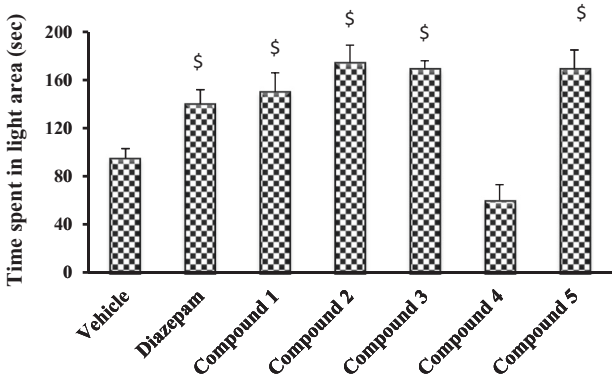

Fig. 2 Time spent in the light area in the dark-light transition test for 3 min. Data analysis was done using one-way ANOVA followed by Bonferroni's multiple comparison's test at $P < 0.05$. $^{\$}$Compared to the vehicle group, $n = 6$. Effect of diazepam and the different compounds on the time spent in the light area in the dark-light transition test

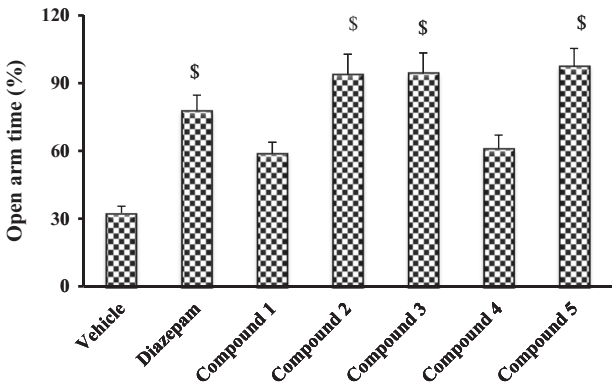

Fig. 3 The percent of open arm time in the elevated plus maze was recorded for 3 min. Data analysis was done using one-way ANOVA followed by Bonferroni's multiple comparison's test at $P < 0.05$. $^{\$}$Compared to vehicle group, $n = 6$. Effect of diazepam and the different compounds on percent time spent in the open arm in the mouse elevated plus maze

Upon a structure-wise argument, please mention why you expect these compounds active while others are not.

Anticonvulsant activity (protection against lethality of pentylenetetrazole)

The test compounds that extended the time to death due to injection of an acute dose of pentylenetetrazole (70 mg/kg) were utilized as an indication for anticonvulsant action.

The use of animal models of seizures is vital for discovering new antiepileptic medications. In the recent years, various new antiepileptic drugs were discovered. Despite these inventions, the search for new more efficacious and tolerable therapies is still crucial (Loscher 2011). The development or discovery of new antiepileptic medications depends greatly on the preclinical experiments using animal

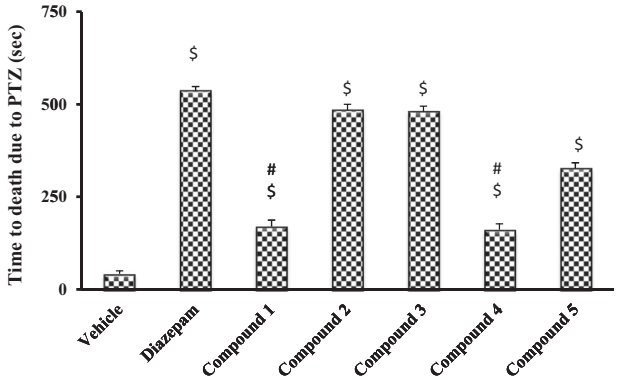

Fig. 4 Time to death after a lethal dose of pentylenetetrazole (70 mg/kg) was recorded. Data analysis was done using one-way ANOVA followed by Bonferroni's multiple comparison's test at $P < 0.05$. $^{\$}$Compared to the vehicle group, $^{\#}$Compared to diazepam group, $n = 6$. Effect of diazepam and the different compounds on the time to death after injection of pentylenetetrazole

models to determine the usefulness before human trials (Steve et al. 2006).

Pentylenetetrazole is a tetrazol derivative that produces stable convulsive behavior in various types of experimental animals. Possible mechanism of action for pentylenetetrazole is to modify chloride ion movement through neuronal membranes. It is known to antagonize the inhibitory neurotransmission by GABA (Jagannatha 2015). Pentylenetetrazole test is an animal model utilized commonly in screening of novel drugs that are efficacious against petit mal epilepsy or absence seizures (White 2003).

In the current experiment, all the test compounds successfully antagonized the lethality of pentylenetetrazole. The time to death recoded with all the test compounds were significantly higher than that recorded in the vehicle group. Furthermore, the effect of compounds **2**, **3**, and **5** was comparable to that produced by diazepam, whereas the effect of compounds **1** and **4** was lower than that produced by diazepam (Fig. 4).

Molecular modeling

We have previously presented the isolation and identification of a ceramide from Red Sea Soft Coral *Sarcophyton auritum* that showed good antiepileptic activity (Eltahawy et al. 2015). The docking experiments performed on this ceramide showed that it is a good modulator to GABA receptors and to a much lower extent to 5HT3 receptors. The newly isolated ceramides are therefore tested for their binding ability to GABA receptors to support the GABA modulation activity as a mode of action for their antiepileptic and anxiolytic activity.

The X-ray crystal structure of a pentameric ion channel gated with a ligand from Erwinia chrysanthemi (ELIC) in

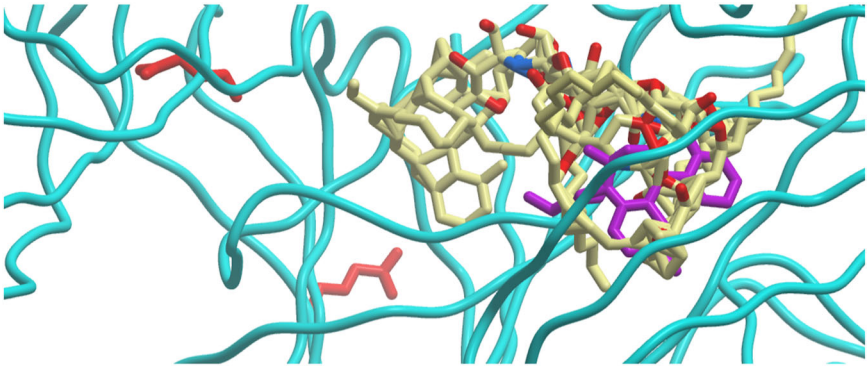

Fig. 5 Ceramide GABA modulators (colored by element) and Flurazepam (violet) bound to GABA allosteric site. Co-crystallized GABA (red) occupying the GABA active sites on the opposite side of the receptors

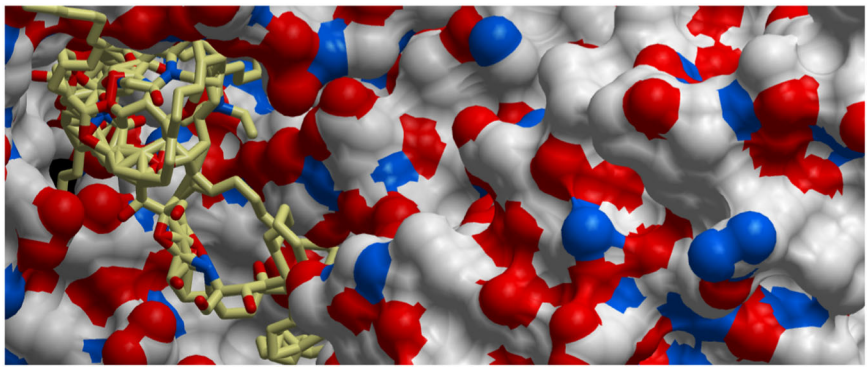

Fig. 6 Ceramide GABA modulators binding to GABA allosteric site represented as an electrostatic potential surface

complex with GABA and flurazepam (PDB code 2YOE) was used in the docking studies. This prokaryotic homolog ELIC is agonized by GABA and is modulated by benzodiazepines and therefore is valid for GABA(A) receptors molecular docking studies.

The docking studies showed that the isolated ceramides are very well interactors and possible modulators of the GABA allosteric site. The docking pattern of all isolated ceramides GABA modulator is very similar in comparative docking to that of the co-crystallized benzodiazepine (flurazepam) suggesting a possible similar mode of action (Fig. 5).

They all lie in the benzodiazepine site and are extended beyond the binding pocket of flurazepam without any steric collision or interference. This leads to our compounds forming more interaction with the benzodiazepine site compared to flurazepam which could potentially make them more active as GABA receptors modulators (Fig. 6).

The docking pattern of all ceramides is very much super imposable and the residues involved in the interactions are very much the same. As an example, ceramide-1 GABA modulator is positioned in the GABA allosteric site and established several interactions including, hydrogen, hydrophobic and electrostatic interactions. Several residues are involved in ligand binding including ILE39, ASN60, ALA 73, PRO74, ALA75, LEU76, PHE78, SER84, PRO85, THR87, GLY88, ASN89, and TYR102. THR87 backbone oxygen is at proximity from the amide NH for possible bonding. TYR 102 is forming hydrogen bonding with one of the sugar secondary OH and the amide carbonyl oxygen (Fig. 7). The tested ceramides are highly flexible molecules and could therefore adopt huge number of conformations for a better interaction with GABA receptors. The long aliphatic side chain is extended in the spacious substrate access channel allowing better search for the best fitting conformation.

In conclusion, the molecular modeling studies performed suggested a CNS depressing activity possibly through a GABA receptor modulation. All compounds lied in the GABA allosteric site with ceramide-1 showing a slightly better interaction based on the hydrogen bonding with THR 87 and TYR 102. The docking results are compatible with the results of the dark-light transition box and the elevated plus maze tests (Puyana et al. 2015).

Acknowledgements The authors are appreciative to R.W.M. van Soest, Faculty of Science, Zoological museum Amsterdam for taxonomic identification of the samples of the sponge. Also thanks are due to the Egyptian Environmental Affairs Agency (EEAA) for facilitating sample collection along the Red Sea coasts.

Compliance with ethical standards

Conflict of interest The authors declare that they have no conflict of interest.

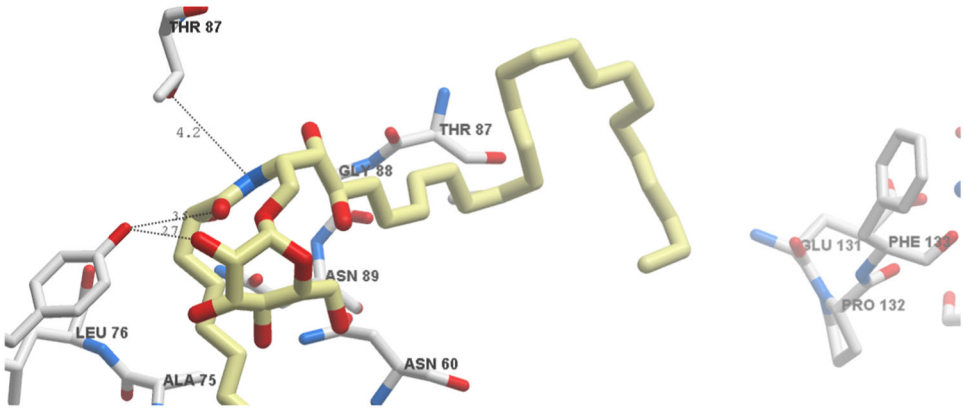

Fig. 7 Ceramide-1 GABA modulator binding to GABA allosteric site; distances in Å are indicated by black lines for potential hydrogen bonding

References

Ahmed, S, Khalifa S, Mesbah M, Youssef D, Hamann, MT (2005) 26th African Health Sciences Congress, Egypt, Abs. 183

Ahmed S, Mesbah M, Youssif D, Khalifa S (2006) Chemical and biological investigations of the Red Sea Sponge Negombata corticata. Bull Pharm Sci (Assuiut University) 29(1):67–75

Ahmed SA, Khalifa SI, Hamann MT (2008) Antiepileptic ceramides from the Red Sea sponge *Negombatacorticata*. J Nat Prod 71:513–515

Beresewicz A, Dobrzyn A, Gorski J (2002) Accumulation of specific ceramides in ischemic/repefused rat heart; effect of ischemic preconditioning. J Physiol Pharmacol 53:371–382

Bieberich E (2012) It's a lipid's world: bioactive lipid metabolism andsignaling in neural stem cell differentiation. Neurochem, Res 37:1208–1229

Chao C, Chou K, Wang G, Wu Y, Wang L, Chen J, Sheu J, Sung P (2010) Norterpenoids and Related Peroxides from the Formosan Marine Sponge *Negombata corticata.* J Nat Prod 73:1538–1543

Cui J, Engelman RM, Maulik N, Das DK (2004) Role of ceramide in ischemic preconditioning. J Am Coll Surg 198:770–777

Eltahawy NA, Ibrahim AK, Radwan MM, Zayton S, Gomaa M, ElSohly MA, Hassanean HA, Ahmed SA (2015) Mechanism of action of antiepileptic ceramide from Red Sea soft coral *Sarcophyton auritum*. BMCL 24:3467–3473

Holmes A, Rodgers RJ (1998) Responses of Swiss-Webster mice to repeated plus-maze experience: further evidence for a qualitative shift in emotional state? Pharmacol Biochem Behav 60(2):473–488

Inagakia M, Isobeb R, Kawanoa Y, Miyamotoa T, Komoria T, Higuchi R (1998) A convergent total synthesis of the michellamines. Eur J Org Chem 63(4):129–131

Izumi E, Ueda-Nakamura T, Veiga Jr VF, Pinto AC, Nakamura CV (2012) Terpenes from Copaifera demonstrated in vitro antiparasitic and synergic activity. Int J Med Chem 55:2994–3001

Jagannatha LokeshShetty (2015) Animal models for pre-clinical antiepileptic drug research. Sci, Technol Dev 34:82–85

Kornhuber J, Müller CP, Becker KA, Reichel M, Gulbins E (2014) The ceramide system as a novel antidepressant target. Trends Pharm Sci 35:293–304

Kubota M, Narita K, Nakkagomi T, Tamura A, Shimasaki H, Ueta N, Yoshida S (1996) Sphingomyelin changes in rat cerebral cortex during focal ischemia. Neurol Res 18:337–341

Kuksis A (Ed.) (1978) Separation and determination of structure of fatty acids. Handbook of lipid research fatty acids and glycerides, Springer, New York, p 1–76

Kwon HC, Lee KC, Cho OR, Jung IY, Cho SY, Kim SY, Lee KR (1991) J Nat Prod 66:466–469

Lecour S, Van der Merne E, Opie LH, Sack MN (2006) Ceramide attenuates hypoxic cell death via reactive oxygen species signaling. J Cardiovasc Pharmacol 47:158–163

Lemieux RU, Von rudlo E (1955) Periodate-permanganate oxidations I. oxidation of olefins. Can J Chem 33:1701–1709

Loscher Wolfgang (2011) Critical review of current animal models of seizures and epilepsy used in the discovery and development of new antiepileptic drugs. Seizure, Eur J Epilepsy 20:359–368

Naderi N, Haghparast A, Saber-Tehrani A, Rezaii N, Alizadeh AM, Khani A, Motamedi F (2008) Interaction between cannabinoid compounds and diazepam on anexiety-like behaviour of mice. *Pharmacol Biochem Behav* 89:64–75

Pellow S, Chopin P, File SE, Briley(1985) Closed arm entries in an elevated plus-maze as a measure of anxiety in the rat. J Neurosci Methods 14(3):149–167

Puyana M, Pawlik J, Plum Finical W (2015) Metabolite variability in Caribbean sponges of the genus. Aplysina 25(6):592–599

Rodgers RJ, Haller J, Halasz J, Mikics N (2003) One trial sensitization to the anxiolytic like effects of cannabinoid receptor antagonist SR141716A in mouse elevated plus maze. Eur J Neurosci 17:1279–1286

Sipkema D, Franssen M, Osinga R, Tramper J, Wijffels R (2005) Marine sponge as pharmacy. Mar Biotechnol l7:142–162

Steve White H, Misty Smith-Yockman, Ajay Srivastava, Karen S Wilcox (2006) Therapeutic assays for the identification and characterization of antiepileptic and antiepileptogenic drugs. Models of seizures and epilepsy, 539–549, Elsevier, Amsterdam

Sugiyama S, Honda M, Higuchi R, Komori T (1991) Stereochemistry of the four diastereomers of ceramide and ceramide lactoside. Liebigs Ann Chem 4:349–356

Sun Y, Xu Y, Liu K, Hua H, Zhu H, Pei Y (2006) Gracilarioside and gracilamides from the Red Alga Gracilaria asiatica. J Nat Prod 69:1488–1491

Torres FA, Passalacqua TG, Velásquez AMA, de Souza RA, Colepicolo P, Graminha MA (2014) New drugs with antiprotozoal activity from marine algae: a review. Rev Bras Farmacogn 24:265–276

Wang G, Beibrich E (2018) Sphingolipids in neurodegeneration (with focus on ceramide and S1P). Adv Biol Regul 70:51–64. https://doi.org/10.1016/j.jbior.2018.09.013. Epub 22 Sep 2018

White HS (2003) Preclinical development of antiepileptic drugs: past, present and future directions. Epilepsia 44:2–8

Xing Y, Tang Y, Zhao L, Wang Q, Qin W, Ji X, Zhang J, Jia J (2016) Associations between plasma ceramides and cognitive and neuropsychiatric manifestations in Parkinson's disease dementia. J Neurol Sci 370:82–87. https://doi.org/10.1016/j.jns.2016.09.028. [PubMed] [CrossRef] [Google Scholar]